Space-time Evolution of Quark-Gluon Plasma Fluid with First Order Phase Transition

Shin Muroya [a,1] and Chiho Nonaka [b,2]

[a] *Tokuyama Women's College, Tokuyama, Yamaguchi, 745 Japan*

[b] *Department of Physics, Waseda University, Shinjuku-ku, Tokyo, 169 Japan*

Abstract

We numerically solve the (3+1)-dimensional relativistic hydrodynamical equation with a bag-model equation of state, which is one of the simplest models for the first order phase transition. Based on the numerical solution, we discuss the space-time evolution of the hot fluid produced in ultra relativistic nuclear collisions. Especially, the space-time structure of the two-phase co-existing region during the quark-gluon plasma-hadron phase transition is analyzed in detail. Finally, we investigate the change of the mass spectra of J/ψ, η_c and ϕ as possible experimental signatures of the phase transition.

Key words: Quark-Gluon Plasma; Hydrodynamical model; Bag model; Mass-shift
PACS: 12.38.Mh, 24.10.Nz, 12.39.Ba, 25.75.-q

1 Introduction

The QCD phase transition and quark-gluon plasma is currently one of the hottest topics in high energy nuclear physics.[1] The recent high performance Lattice simulation suggests that the order of the QCD phase transition in the real world, i.e. 2 massless quarks and 1 massive quark case, is first order.[2] If the QCD phase transition is of the first order, the latent heat will be released at the phase transition temperature T_c and an isothermal Quark-Gluon Plasma(QGP)-hadron co-existing region will appear in the case that the change of the whole system is slower than the microscopic relaxation time. If

[1] E-mail : muroya@yukawa.kyoto-u.ac.jp
[2] E-mail : 696l0906@mn.waseda.ac.jp

such a scenario will be realized, the space time volume of the $T = T_c$ region can become significantly large, and physical quantities which are characteristic to the phase transition temperature T_c will be available as the experimental signatures of the phase transition. The purpose of this paper is to investigate how large a region with $T = T_c$ will be produced at the CERN SPS experiment and how clearly the hadronic mass shift at finite temperature can work as possible signatures of the phase transition.

As an equation of the state, we here adopt the bag model which is one of the simplest models for the first order phase transition. The hydrodynamical model for the QGP fluid has already been discussed in many papers since Bjorken first introduced the simple scaling model in 1+1 dimensional expansion[3]. We discussed 1+1 dimensional expansion of the viscous fluid [4] and 3+1 dimensional expansion with phase transition[5]. Based on the hydrodynamical model, we also discussed electromagnetic probe of QGP[6]. As concerns the treatment of the first order phase transition, Alam et al. and Kajantie et al. [7] focused their discussion only on the transverse expansion based on the scaling ansatz. Sollfrank et al. [8] discussed a smeared equation of state with a small temperature width. In order to focus our discussion to the $T = T_c$ region, we solved 3+1 dimensional expansion keeping an equation of state with the exact first order phase transition.

Experimentally, at SPS energy, net baryon number is not negligible even in the central region. In order to take correctly account of the baryon number conservation law, we must solve the coupled equations of hydrodynamics and baryon current conservation[9]. However, if we adopt baryon number independent of an equation of state, the dynamics of the four velocity is free from the baryon conservation law and the role of the chemical potential is only for the calculation of the baryon number at the final stage[10]. Therefore, we may say that the baryon free fluid model works well enough in the discussion of space time evolution of the fluid with the simple bag model.

The mass shift of the hadrons in the hot medium is believed to be a promising detectable signature of the high temperature region. Hioki et al. proposed J/ψ and η_c [11] and Asakawa et al. proposed ϕ as the possible probe[12]. Following their discussions, we apply our hydrodynamical model to the evaluation of the mass spectrum of these particles.

2 Hydrodynamical Equation

Assuming cylindrical symmetry to the system, we introduce cylindrical coordinate τ, η, r and ϕ instead of the usual Cartesian coordinate x, y, z and t, where,

$$
\begin{aligned}
t &= \tau \cosh \eta, \\
z &= \tau \sinh \eta, \\
x &= r \cos \phi, \\
y &= r \sin \phi.
\end{aligned} \tag{1}
$$

The four velocity U^μ is given as,

$$
\begin{aligned}
U^t &= U^\tau \cosh \eta + U^\eta \sinh \eta, \\
U^z &= U^\tau \sinh \eta + U^\eta \cosh \eta, \\
U^x &= U^r \cos \phi + U^\phi \sin \phi, \\
U^y &= U^r \sin \phi - U^\phi \cos \phi.
\end{aligned} \tag{2}
$$

Taking into account $U^\mu U_\mu = 1$ and cylindrical symmetry, U^μ can be represented with two variables Y_{L} and Y_{T},

$$
\begin{aligned}
U^\tau &= \cosh Y_{\mathrm{T}} \cosh(Y_{\mathrm{L}} - \eta), \\
U^\eta &= \cosh Y_{\mathrm{T}} \sinh(Y_{\mathrm{L}} - \eta), \\
U^r &= \sinh Y_{\mathrm{T}}, \\
U^\phi &= 0.
\end{aligned} \tag{3}
$$

As is well known, the relativistic hydrodynamical equation is given as,

$$
\partial_\mu T^{\mu\nu} = 0, \tag{4}
$$

and the energy momentum tensor of perfect fluid is given by,

$$
T^{\mu\nu} = E U^\mu U^\nu - P(g^{\mu\nu} - U^\mu U^\nu). \tag{5}
$$

where E and P are energy density and pressure, respectively. Usually, thermodynamical quantities such as E and P are treated as local quantities through temperature $T = T(x^\mu)$.

In order to solve the above hydrodynamical equation, we need an equation of state. In this paper, we adopt the bag model equation of state as the simplest model for the QCD phase transition of first order. In the bag model, thermodynamical quantities below the phase transition temperature correspond to those of a massive hadronic gas. On the other hand, in the high temperature phase, thermodynamical quantities are given by those of massless QGP gas with bag constant B. In this paper, we assumed pions and kaons in the hadronic phase and u-, d-, s-quarks and gluons in the QGP phase. Putting the phase transition temperature, $T_{\mathrm{c}} = 160$ MeV, into the condition of pressure continuity, we can obtain the bag constant as $B = 412$ MeV/fm^3.

At the phase transition temperature T_c, pressure P is continuous but other quantities such as energy density E and entropy density S have discontinuity as a function of temperature. We parameterize these quantities during the phase transition by using the volume fraction λ [11]. We assume that thermodynamical quantities at $T = T_\mathrm{c}$ are the functions of the space-time point through $\lambda(x^\mu)$ and given as,

$$\begin{aligned} E(\lambda) &= \lambda E_\mathrm{qgp}(T_\mathrm{c}) + (1-\lambda) E_\mathrm{had}(T_\mathrm{c}), \\ S(\lambda) &= \lambda S_\mathrm{qgp}(T_\mathrm{c}) + (1-\lambda) S_\mathrm{had}(T_\mathrm{c}), \end{aligned} \tag{6}$$

where $0 \leq \lambda(x^\mu) \leq 1$. This parameterization enables us not only to solve the hydrodynamical equation easily but also to estimate hadronic fraction in the phase transition region for later use.

3 Space-time evolution of co-existing region

Assuming that local equilibrium is achieved at 1 fm later than the collision instance, we give initial conditions of the hydrodynamical model on the $\tau = \tau_0 = 1$ fm hypersurface. Initial entropy density distribution is given as,

$$S(\tau_0, \eta) = S(T_0) \exp\left(-\frac{(|\eta| - \eta_0)^2}{2 \cdot {\sigma_\eta}^2} \theta(|\eta| - \eta_0) - \frac{(r - r_0)^2}{2 \cdot {\sigma_r}^2} \theta(r - r_0)\right), \tag{7}$$

and parameters we used in this paper are summarized in table 1.

Table 1. Initial Parameters

	T_0 (MeV)	η_0	σ_η	r_0 (fm)	σ_r (fm)
S + Au	209	0.7	0.7	$(32)^{(1/3)} - 1.0$	1.0
Pb + Pb	190	0.7	1.0	$(197)^{(1/3)} - 1.0$	1.0

Putting freeze-out temperature as $T_\mathrm{f} = 140$ MeV for S+Au and $T_\mathrm{f} = 138$ MeV for Pb+Pb, respectively, we can reproduce hadronic distributions of the recent experimental results. Figure 1 and fig. 2 show the pseudo-rapidity distribution of charged hadrons and the transverse momentum distribution of neutral pions, respectively. Data for S+Au 200 AGeV collisions are obtained by WA80[13,14] and data of Pb+Pb 158 AGeV collisions are obtained by NA49[15] (rapidity distribution of charged hadrons) and WA98 [16] (transverse momentum distribution of neutral pions).

Figure 3 displays the space time evolution of the temperature distribution in the Pb+Pb case. The isothermal region at phase transition temperature $T =$

T_c appears very clearly. The structure of temporal evolution does not differ essentially from the case of smooth phase transition in a small temperature region [5,8]. By virtue of the use of the volume fraction λ at phase transition temperature, we can pick up the volume element with the temperature at just the phase transition point. The temperature profile function (fig. 4) shows the significant contribution of the space-time volume at $T = T_c$.

4 Change of the mass spectrum

As a signal of the hot hadronic region, shifted J/ψ mass-spectrum and η_c were proposed by Hioki et al.[11] and ϕ by Asakawa et al.[12] In these papers, authors discussed possible signals based on a scaling hydrodynamical model. We apply our (3+1)-dimensional hydrodynamical model to these calculation and investigate numerically how clear the shifted hadronic mass spectra appear in the present CERN SPS case.

According to ref. [11], the invariant mass distribution of leptonic pair decay is given by

$$\frac{1}{\sigma}\frac{\mathrm{d}\,\sigma}{\mathrm{dM}} = \int_{T_f}^{T_0} \mathrm{d}\,T \Phi(T) n(T) \Gamma_{l\bar{l}}(T) \delta(M - M(T)),$$

where Φ is the temperature profile function which we have already calculated in the previous section. In ref. [11], Hioki et al. evaluated shifted mass $M(T)$ and decay width $\Gamma_{l\bar{l}}(T)$ based on a c-$\bar{\mathrm{c}}$ potential model and we also use their result here. Charmonium density $n(x^\mu)$ was estimated by the kinetic equation in ref. [11], and we adopt Maxwell-Boltzmann distribution for $n(x^\mu)$, that is,

$$n(T) = 3\left(\frac{MT}{2\pi}\right)^{\frac{3}{2}} \exp(-\frac{M}{T}),$$

for simplicity. However, charmonium mass is much larger than the typical temperature of the fluid, above $n(T)$ is almost constant and final results were dominated by the temperature profile function $\Phi(T)$. Figure 5 and 6 show the possible J/ψ and η_c spectrum for the CERN SPS experiment in comparison with the results of ref. [11]. In fig. 5, "critical" and "thermal" correspond to the yields of $T = T_c$ and $T_f < T < T_c$, respectively. "Cold" in fig. 5 is given by,

$$\frac{1}{\sigma}\frac{\mathrm{d}\,\sigma}{\mathrm{d}\,M} = \frac{N\Gamma_{l\bar{l}}(T=0)}{\Gamma_{\mathrm{total}}}\delta(M - M(T))$$

which corresponds to the naive thermal contribution from the freeze-out hypersurface. Note that, in order to make comparison clear, the results of ref. [11], which are the (1+1)-dimensional calculation, were so normalized in fig. 5 and fig. 6 as to give the same "cold" contribution to our results. In fig. 5 and

fig. 6, quantitative difference between S+Au and Pb+Pb is consistent with the difference in the temperature profile functions (fig. 4).

The yield of J/ψ from $T_{\rm c}$ is several orders smaller compared to the cold and thermal J/ψ. However, the situation of η_c is much better than J/ψ: in our results, η_c from the $T = T_{\rm c}$ region is almost the same order as the others. Hence, η_c will be a better signature of $T = T_{\rm c}$ than J/ψ. These results are consistent with ref. [11]. Because of the very small decay width of J/ψ and η_c, changes of the mass seem very clear and easy to detect. On the other hand, their life time is much longer than the hot fire ball and the number of particles which decay in the hot medium is very small. Therefore, shifted η_c and J/ψ are hardly detectable in the present experimental situation, but in future experiments with high precision, these can work as good signals.

Asakawa et al.[12] started their discussion from the number of particles which decay in unit time and unit phase space which is given as,

$$\mathrm{d}\ N = \frac{g_\phi}{(2\pi)^3}\frac{1}{\gamma}\Gamma_{\bar{l}l}(T)\,\mathrm{e}^{-p^\mu U_\mu/T}\,\mathrm{d}\ ^4x\mathrm{d}\ ^3p, \tag{8}$$

where g_ϕ is the degeneracy of ϕ and γ is the Lorentz factor of a moving particle. They imported the results of the QCD sum rule for the decaying constant in finite temperature, $\Gamma(T)$. From (8) we obtain

$$\frac{\mathrm{d}\ N_{\bar{l}l}}{\mathrm{d}\ M\mathrm{d}\ y} = \frac{g_\phi}{(2\pi)^3}\iint \frac{1}{\gamma}\Gamma_{\bar{l}l}(T)F_\phi(M, m_\phi(T))\mathrm{e}^{-p^\mu U_\mu/T}\mathrm{d}\ ^4x\mathrm{d}\ p_T\mathrm{d}\ p_T\mathrm{d}\ \varphi, \tag{9}$$

where $F_\phi(M, m_\phi(T))$ is the normalized smearing function to take account of experimental resolution. $F_\phi(M, m_\phi(T))$ is assumed to have a Gaussian form,

$$F_\phi(M, m_\phi(T)) = \frac{1}{\sigma\sqrt{2\pi}}\mathrm{e}^{-(M-m_\phi(T))^2/2\sigma^2}, \tag{10}$$

where σ is put as 10 MeV. With use of the above formula, we evaluate the ϕ spectrum based on our hydrodynamical model. Figure 7 shows the ϕ spectrum from S+Au and Pb+Pb collisions at CERN SPS energy. The dashed line in Fig. 7 stands for the contribution of $T = T_{\rm c}$ and the dotted line for the ϕ from the hot hadronic region. Quantitative difference between yields in S+Au(a) and Pb+Pb(b) are almost proportional to the difference in the temperature profile functions(fig. 4). Comparing to S+Au, the ratio of the peak around 959 MeV to the one around 1020 MeV is large in the Pb+Pb case.

These curves show clear difference as we expected, but the accumulated result (solid line) does not show distinguishable double peaks. In the accumulated results, we can find clear double peaks originating from the cold component and

hot hadronic contribution, however it would not mean directly the existence of the QCD phase transition.

5 Concluding remarks

We solved a (3+1)-dimensional hydrodynamical model with first order phase transition model(bag model). We can parameterize our hydrodynamical model so as to reproduce well the present experimental hadron spectrum. Based on the numerical solution we discussed the space-time structure of the isothermal region at phase transition $T = T_{\rm c}$, which appears as a sharp peak in the temperature profile function. Applying our numerical solution, we evaluated mass spectra of J/ψ, $\eta_{\rm c}$ and ϕ which have been proposed as possible signals for the existence of an isothermal $T = T_{\rm c}$ region. According to our numerical investigation, if the experimental resolution is as good as $\sigma = 10$ MeV, we may have a chance to find the double-peak of the ϕ spectrum, but in the present CERN SPS Pb+Pb experiment, $T = T_{\rm c}$ peak is indistinguishable from the hot hadronic contribution.

We are indebted to Prof. I. Ohba and Prof. H. Nakazato for their helpful comments and their continuous encouragement. We thank many discussions between Dr. H. Nakamura, Dr. T. Hirano and other members of Waseda Univ. high energy physics group. We also thank Dr. T. Peitzmann and Dr. S. Nishimura for discussions about the recent WA98 results. Numerical analyses have been done with workstations of Waseda Univ. high energy physics group.

References

[1] See, for example, *Proceedings of Quark Matter '96*, *Nucl. Phys.*A610 (1996)1c.

[2] K. Kanaya, *Nucl. Phys.* **B**(Proc. Supple.)**47**(1996)144; K. Kanaya in the Proceedings of the Third International Conference of the Physics and AstroPhysics of Quark-Gluon Plasma(held at Jaipool, India (1997)).

[3] J. D. Bjorken, Phys. Rev. **D27**(1983)140.

[4] Y. Akase, S. Daté, M. Mizutani, S. Muroya, M. Namiki and M. Yasuda, *Prog. Theor. Phys.* **82**(1989)591.

[5] Y. Akase, M. Mizutani, S. Muroya and M. Yasuda, *Prog. Theor. Phys.* **85** (1991)305; S. Muroya, H. Nakamura and M. Namiki, *Prog. Theor. Phys. Suppl.* **No.120**(1995)209.

[6] T. Hirano, S. Muroya and M. Namiki *Prog. Theor. Phys.* **98**(1997)129

[7] J. Alam, S. Raha and B. Sinha, *Phys. Rep.* **273**(1996)243; J. Alam, D. K. Srivastava, B. Sinha and D. N. Basu, *Phys. Rev.* **D48**(1993)1117; K. Kajantie, M. Kataja, L. McLerran and P. V. Ruuskanen, Phys. Rev. **D34**(1986)811.

[8] J. Sollfrank, P. Houvinen, M. Kataja, P. V. Ruuskannen, M. Prakash and R. Venugopalan, *Phys. Rev.* **C55**(1997)391.

[9] T. Ishii and S. Muroya, *Phys. Rev.* **D46**(1992)5156.

[10] N. Arbex; U. Ornik, M. Plümer, A. Timmermann and R. M. Weiner, *Phys. Lett.***B345**(1995)307. U. Ornic, M. Plümer, B.R. Schlei, D. Strottman, and R.M. Weiner, *Phys. Rev.* **D54**(1996)1381.

[11] S. Hioki, T. Kanki and O. Miyamura, Phys. Lett. **B 261**(1991)5; T. Hashimoto, K. Hirose, T. Kanki and O. Miyamura, Z. Phys. **C38** (1988)251.

[12] M. Asakawa and C. M. Ko, Phys. Lett. **B 322**(1994)33.

[13] R. Albrecht et al. : WA80, *Z. Phys.* **C55**(1992)539.

[14] R. Santo et al. : WA80, *Nucl. Phys.* **A566**(1994)61c.

[15] S. V. Afanasiev et al. :NA49, *Nucl. Phys.* **A610**(1996)188c.

[16] M. Aggarwal et al. : WA98, *Nucl. Phys.* **A610**(1996)200c; T. Peitzmann, private communication.

Figure Caption

Figure1:(a) Pseudo-rapidity distribution of charged hadrons in S+Au 200 AGeV collision in comparison with the data of CERN WA80, and (b) rapidity distribution of charged hadrons in Pb+Pb 158 AGeV collision in comparison with the data of CERN NA49.

Figure2:Transverse momentum distribution of neutral pions in S + Au collision 200 AGeV collision in comparison with the data of CERN WA80(a), Pb+Pb 158 AGeV collision in comparison with the data of CERN WA98(b).

Figure3:The space-time evolution of the temperature-distribution of the Pb+Pb 158 AGeV collision. Initial temperature is 190 MeV, critical temperature is 160 MeV and freeze-out temperature is 138 MeV. The flat area corresponds to the mixed phase. From these graphs we can see that the QGP phase vanishes at $\tau = 2.0$ fm and the mixed phase vanishes at $\tau = 8.5$ fm and at $\tau = 11.5$ fm the temperature becomes lower than the freeze-out temperature everywhere in the fluid.

Figure4:The temperature profile function of S+Au 200 AGeV collision(a) and Pb+Pb 158 AGeV collision(b). The sharp peak at critical temperature corresponds to the huge space-time size of the mixed phase region which is caused by the released latent heat.

Figure5:The invariant mass distribution of lepton pairs from mass-shifted J/ψ in the hadronic phase of "critical","thermal" and "cold" in S+Au collision(a) and Pb+Pb collision(b). The dashed line and a square point with a dot stand for the results obtained by Hioki et al. In these figures, to make comparison clear, the results of Hioki et al. were so normalized as to give the same "cold" contribution to our results.

Figure6:The invariant mass distribution of photon pairs from mass-shifted η_c in the hadronic phase of "critical","thermal" and "cold" in S+Au collision(a) and Pb+Pb collision(b). The dashed line and a square point with a dot stand for the results of Hioki et al. In order to make comparison clear, the results of Hioki et al. were so normalized as to give the same "cold" contribution to our results.

Figure7:The invariant mass distribution of lepton pairs from mass-shifted ϕ in the central rapidity region in S+Au collision(a) and Pb+Pb collision(b). The dashed line stands for the contribution from the mixed phase, the dotted line for the hadronic phase, the chained line for the contribution from the freeze-out hypersurface and the solid line for the total contribution, respectively. The peak at 1020 MeV corresponds to the contribution from the freeze-out hypersurface.

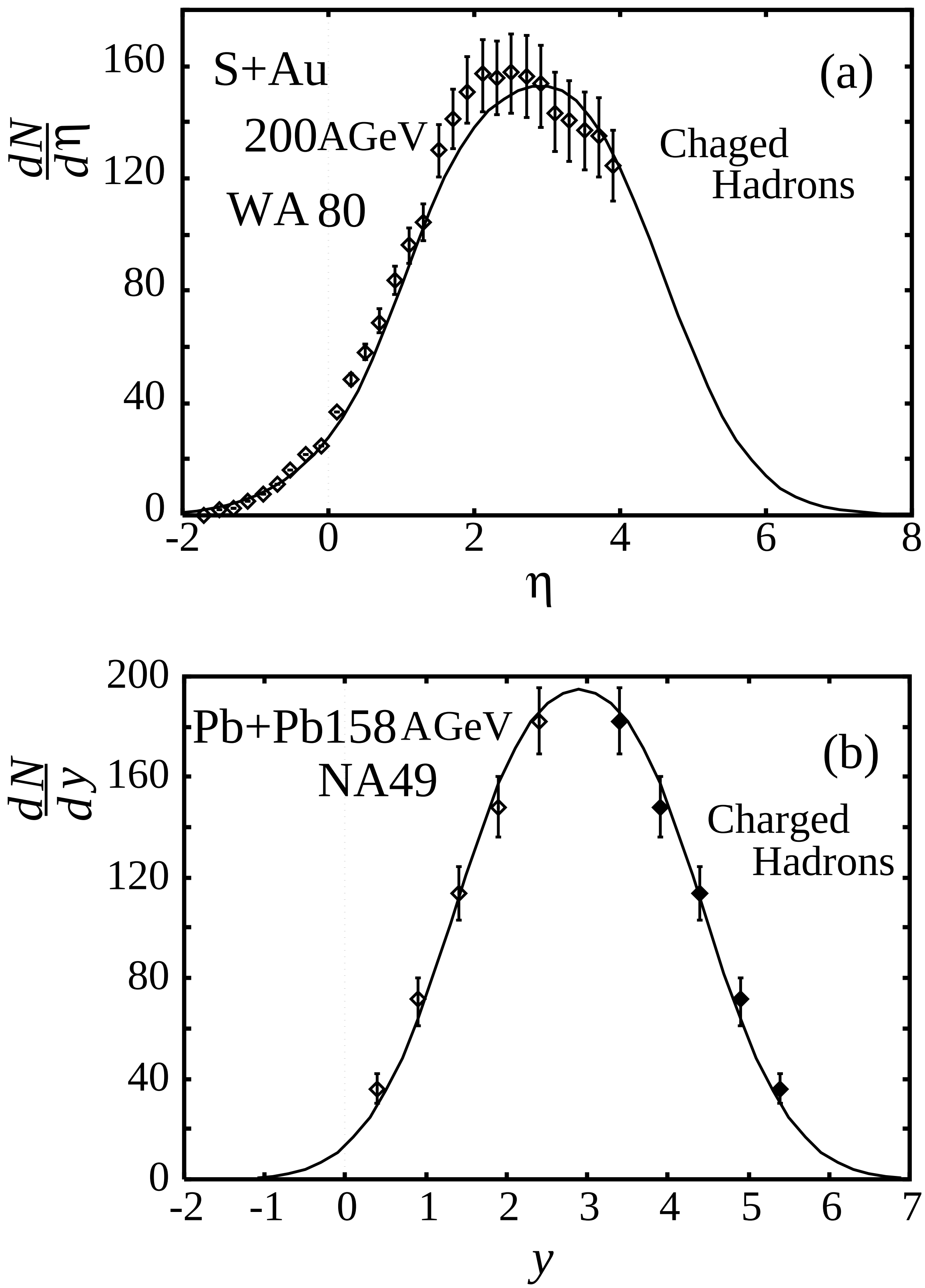

S+Au
200AGeV
WA 80
(a)
Chaged
Hadrons
$\frac{dN}{d\eta}$
η
Pb+Pb158AGeV
NA49
(b)
Charged
Hadrons
$\frac{dN}{dy}$
y

Fig. 1

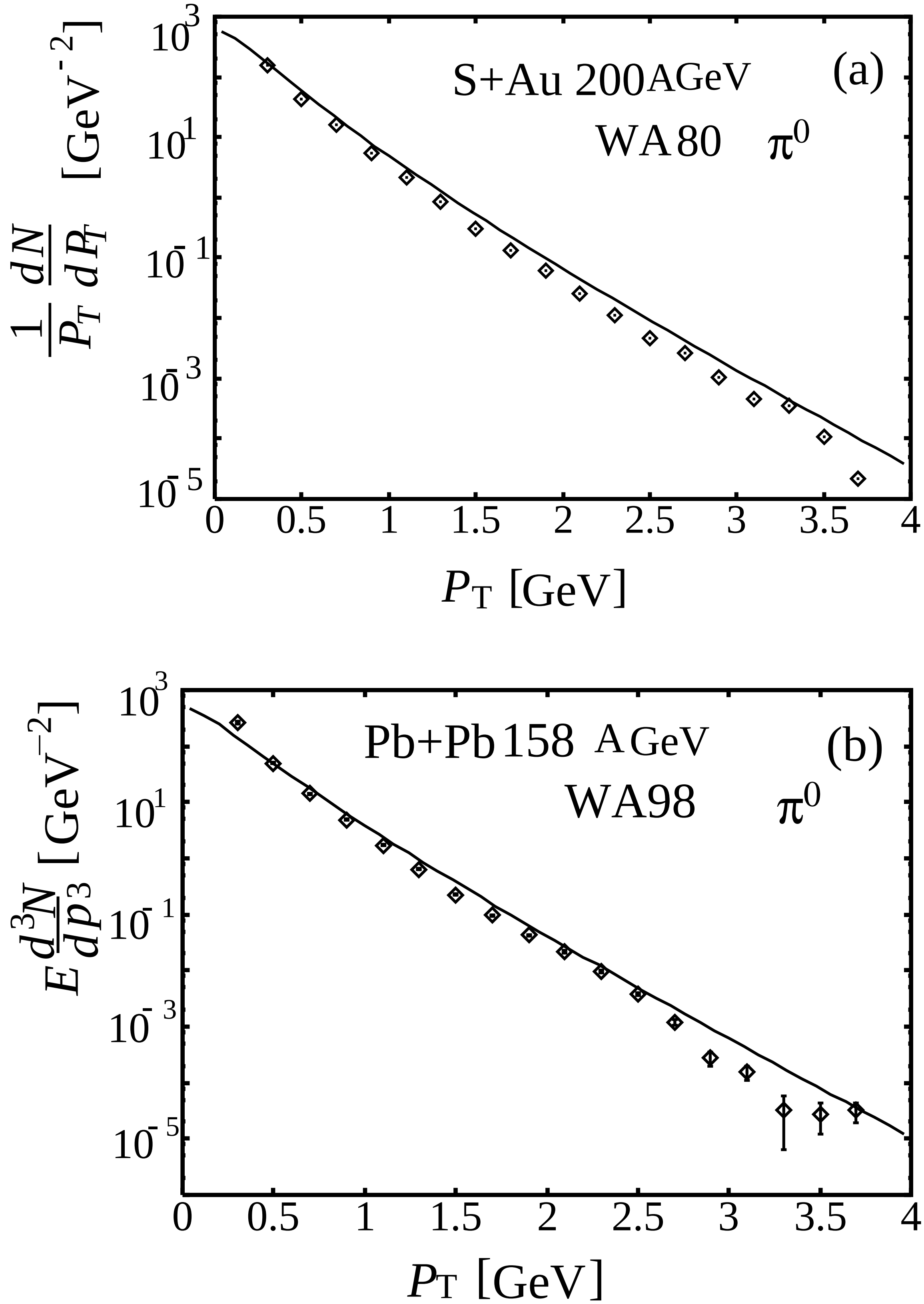
S+Au 200AGeV
(a)
WA80 π0
$\frac{1}{P_T}\frac{dN}{dP_T}$ [GeV^{-2}]
P_T [GeV]
Pb+Pb 158 AGeV
(b)
WA98 π0
$E\frac{d^3N}{dp^3}$ [GeV^{-2}]
P_T [GeV]

Fig. 2

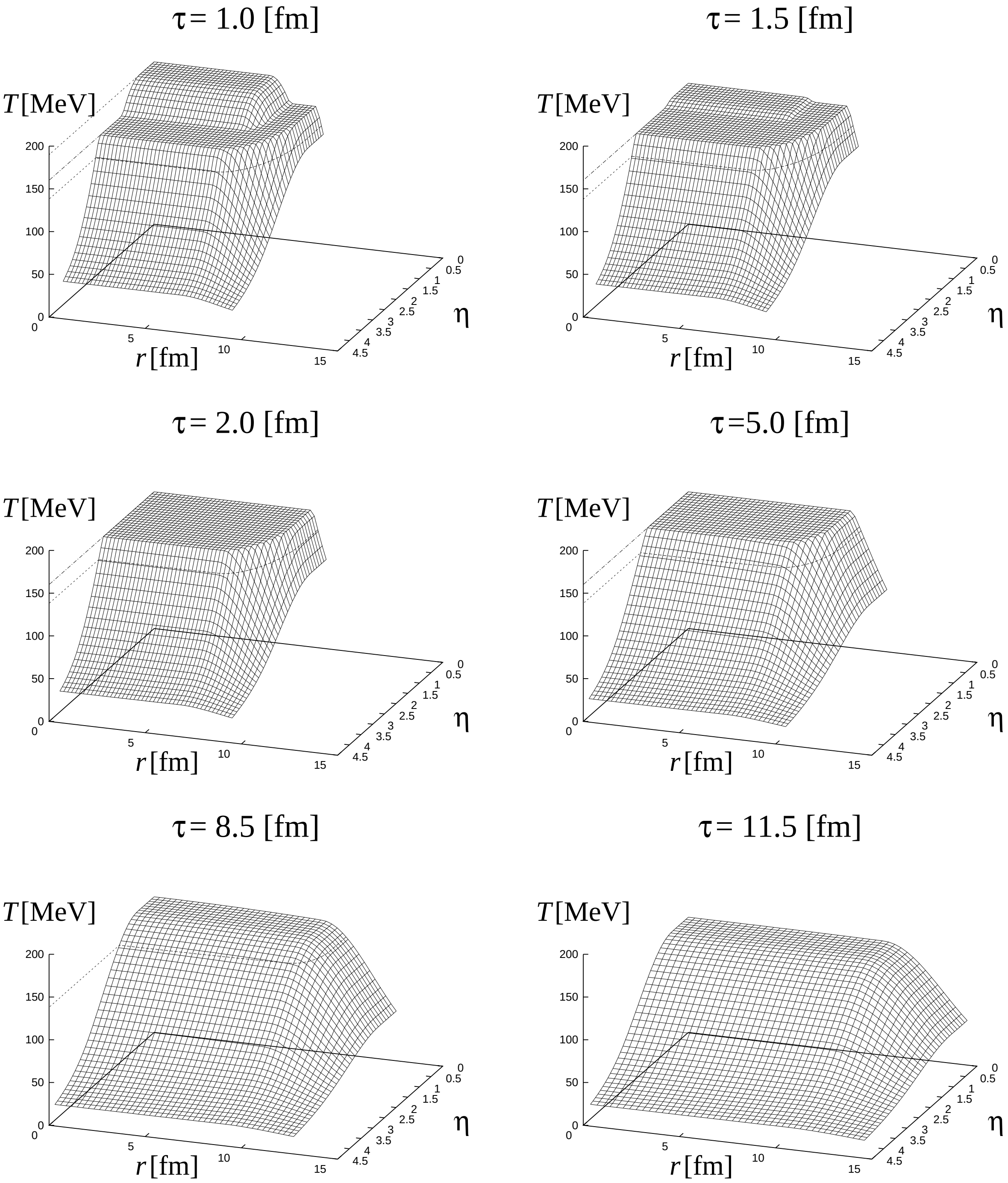

Fig. 3

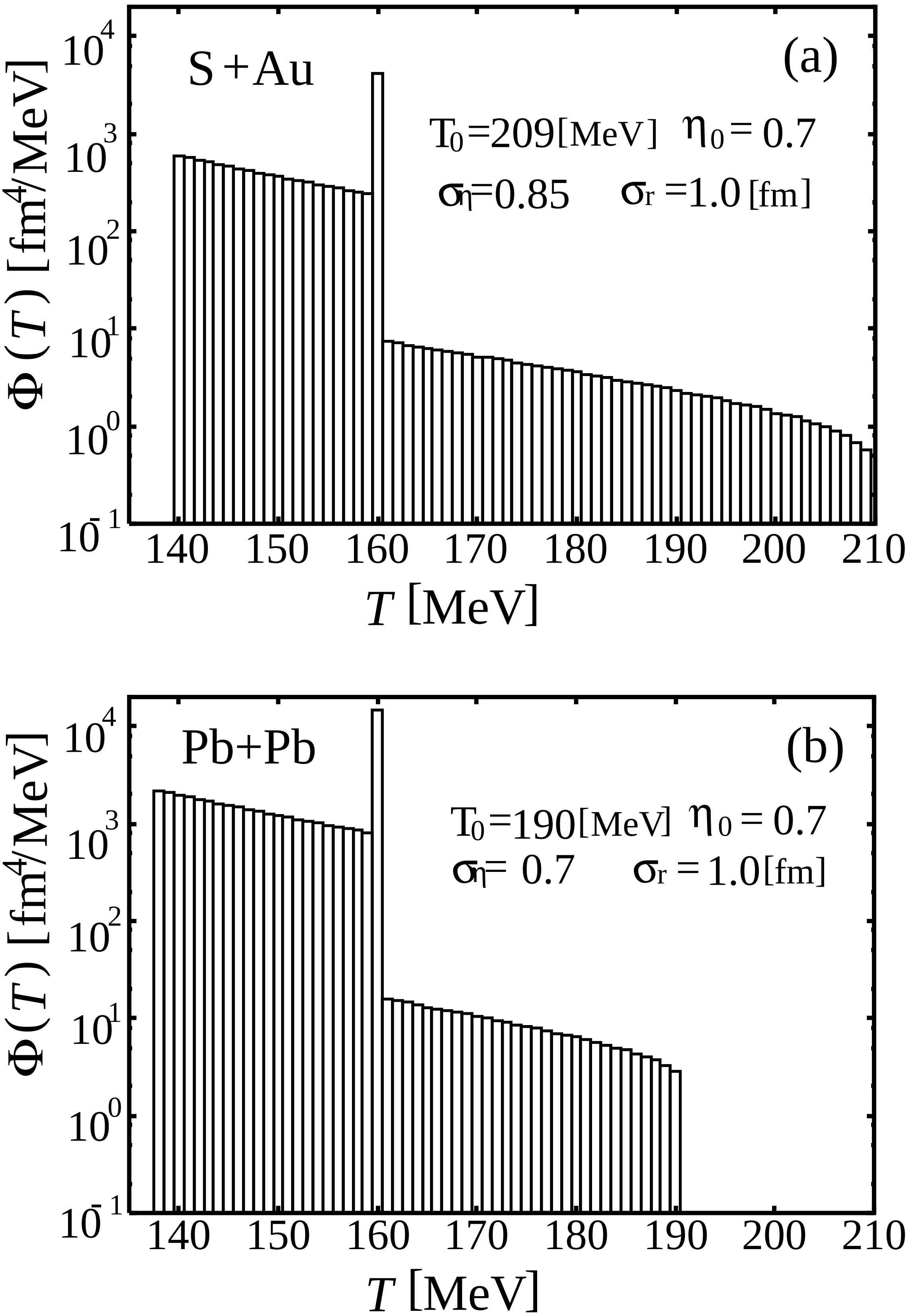
S + Au
(a)
T0=209[MeV] η0 = 0.7
ση=0.85 σr =1.0 [fm]
Pb+Pb
(b)
T0=190[MeV] η0 = 0.7
ση= 0.7 σr = 1.0[fm]
Φ(T) [fm4/MeV]
T [MeV]
10-1
100
101
102
103
104
140
150
160
170
180
190
200
210

Fig. 4

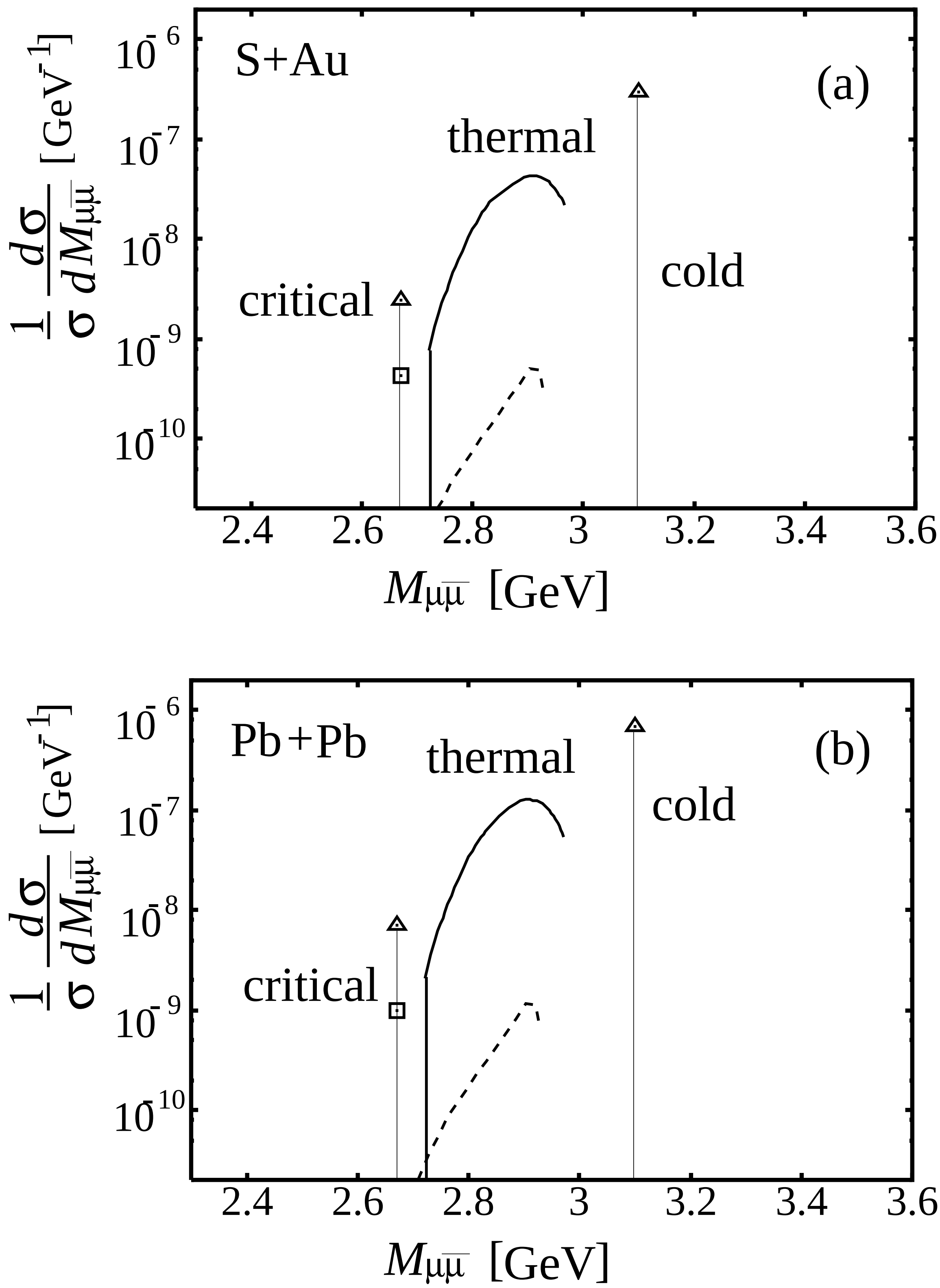
S+Au
(a)
thermal
critical
cold
Pb+Pb
(b)
2.4
2.6
2.8
3
3.2
3.4
3.6
$M_{\mu\bar{\mu}}$ [GeV]
$\frac{1}{\sigma}\frac{d\sigma}{dM_{\mu\bar{\mu}}}$ [GeV^{-1}]
10^{-6}
10^{-7}
10^{-8}
10^{-9}
10^{-10}

Fig. 5

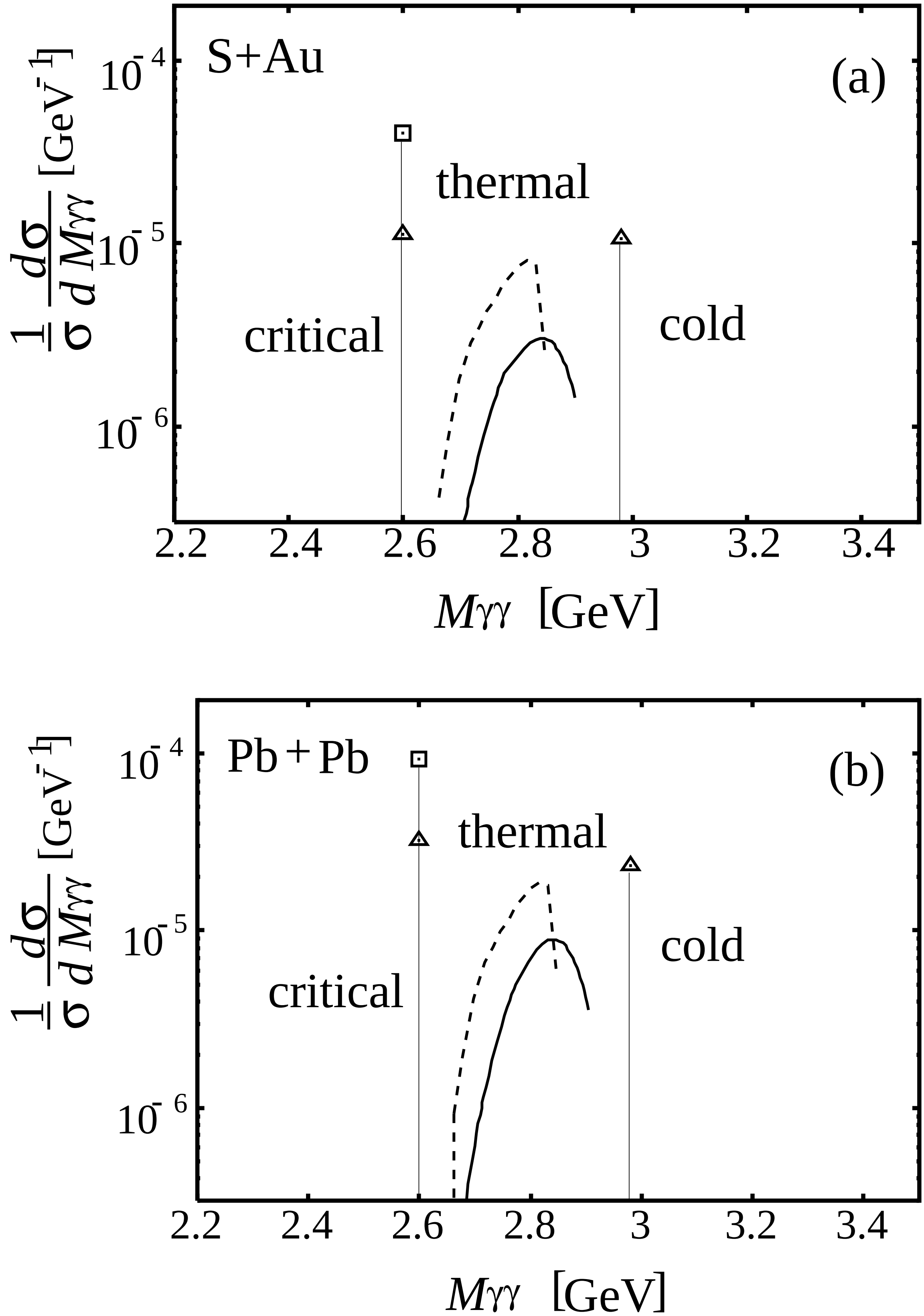
S+Au
(a)
thermal
critical
cold
2.2 2.4 2.6 2.8 3 3.2 3.4
Mγγ [GeV]
Pb+Pb
(b)
thermal
critical
cold
2.2 2.4 2.6 2.8 3 3.2 3.4
Mγγ [GeV]

Fig. 6

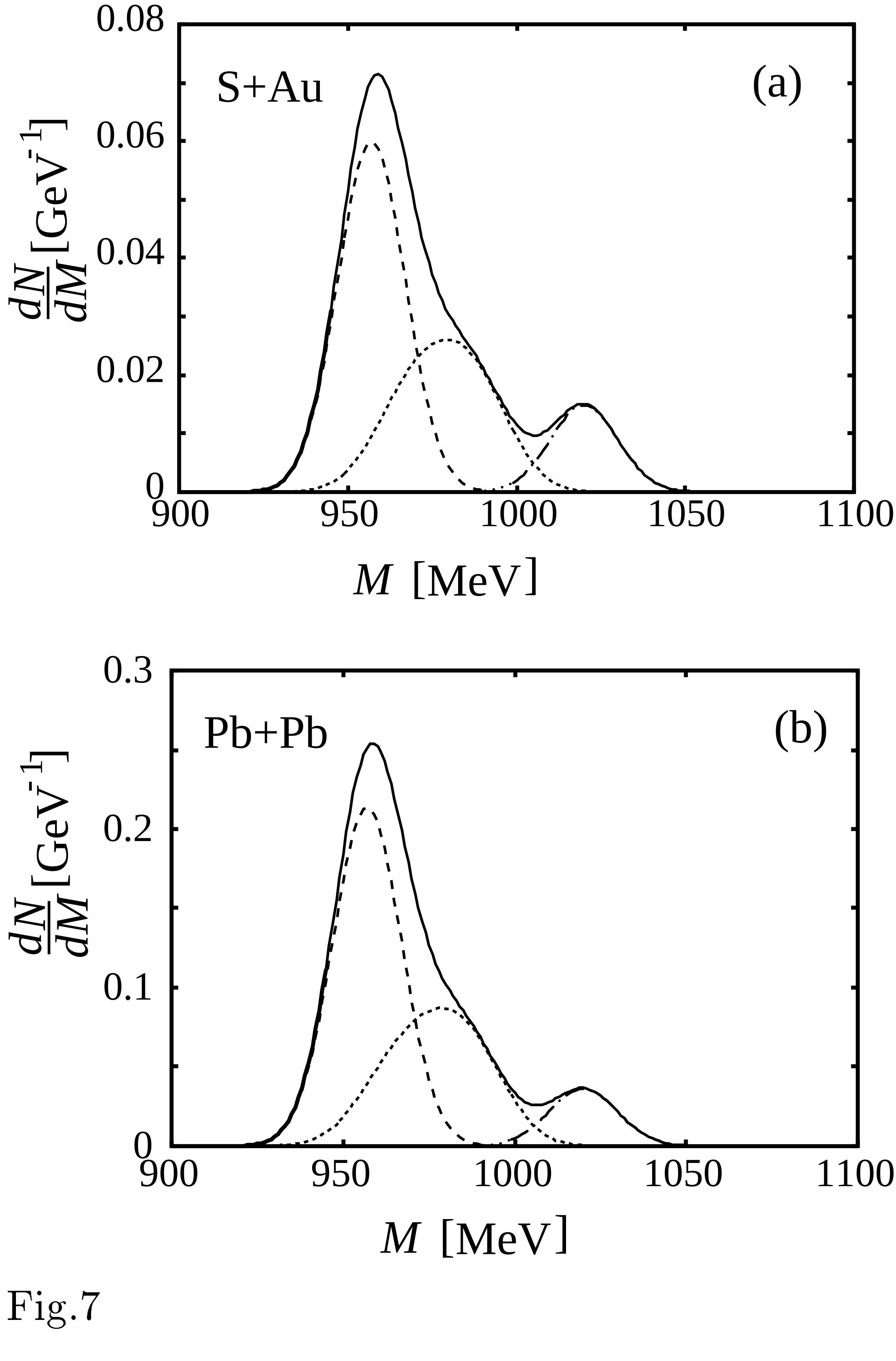
S+Au
(a)
dN/dM [GeV-1]
0.08
0.06
0.04
0.02
0
900
950
1000
1050
1100
M [MeV]
Pb+Pb
(b)
dN/dM [GeV-1]
0.3
0.2
0.1
0
900
950
1000
1050
1100
M [MeV]

Fig.7